

# Muon Fluxes from Dark Matter Annihilation

Arif Emre Erkoca,<sup>1</sup> Mary Hall Reno,<sup>2</sup> and Ina Sarcevic<sup>1,3</sup>

<sup>1</sup>*Department of Physics, University of Arizona, Tucson, AZ 85721*

<sup>2</sup>*Department of Physics and Astronomy, University of Iowa, Iowa City, IA*

<sup>3</sup>*Department of Astronomy and Steward Observatory, University of Arizona, Tucson, AZ 85721*

We calculate the muon flux from annihilation of the dark matter in the core of the Sun, in the core of the Earth and from cosmic diffuse neutrinos produced in dark matter annihilation in the halos. We consider model-independent direct neutrino production and secondary neutrino production from the decay of taus produced in the annihilation of dark matter. We illustrate how muon energy distribution from dark matter annihilation has a very different shape than muon flux from atmospheric neutrinos. We consider both the upward muon flux, when muons are created in the rock below the detector, and the contained flux when muons are created in the (ice) detector. We contrast our results to the ones previously obtained in the literature, illustrating the importance of properly treating muon propagation and energy loss. We comment on neutrino flavor dependence and their detection.

## I. INTRODUCTION

The dark matter problem, where more matter is required to account for gravitational forces observed on astronomical objects than it is visible, has persisted for more than seven decades [1]. Observations of galactic rotation curves [2], orbital velocities of galaxies within clusters [3], anisotropies of the cosmic microwave background (CMB) [4], distance measurements from Type Ia supernovae (SN) and baryon acoustic oscillations (BAO) [5], and large scale structure [6] all imply the existence of cold (non-relativistic) dark matter (CDM) with an abundance of 23% of the total density of the Universe ( $\Omega_{CDM} = 0.233 \pm 0.013$ ). In addition, the combination of the CMB, SN and BAO data predicts that only 4% of the total density of the Universe can be attributed to the baryonic matter ( $\Omega_{baryons} = 0.0462 \pm 0.0015$ ). Thus, the particle content of the CDM can not be explained in the context of the standard model.

In all extensions of the standard model, there are many candidates to account for CDM: weakly interacting massive particles (WIMPs), axions, superheavy dark matter (WIMPZILLAs), and solitons (Q-balls) [1, 7, 8, 9] to name a few. Among these possibilities, a WIMP of mass of order 100 GeV provides a natural explanation for the observed density of dark matter today [10, 11]. These WIMPs were abundant and in thermal equilibrium in the early Universe and then eventually “froze out” due to the Hubble expansion.

An interesting coincidence, independent of the dark matter issue, is that the 100 GeV scale is the characteristic scale of new physics beyond the standard model according to naturalness arguments [12]. Collider experiments such as the Large Hadron Collider (LHC) at CERN will explore this new scale physics in the near future [13]. The detection and characterization of dark matter particles is possible in these LHC searches. However, the LHC experiments will not be able to determine detailed properties of these particles such as whether they are stable and what their couplings are to other particles.

Apart from the colliders, there are two independent

but complementary approaches to search for dark matter: direct and indirect detection [14], including dark matter accumulation in the Earth and Sun [15, 16, 17] and in the galactic center [18], and subsequent annihilation to neutrinos [19, 20, 21, 22]. There are a number of direct detection experiments [23, 24, 25, 26]. Direct searches can provide valuable data on the dark matter’s couplings to the standard model. They all look for energy deposition via nuclear recoils from WIMP scattering by using different target nuclei and detection strategies, and expect to observe the same WIMP mass and cross sections. Currently, the strongest upper bounds ( $\sim 10^{-7}$ pb) on the spin independent WIMP-nucleon cross section of a WIMP with mass  $\sim 100$  GeV come from the **XENON** Dark Matter Search (XENON) [24] and the **Cryogenic Dark Matter Search** (CDMS) [25] experiments. So far, contrary to the null results of all other direct searches, the **DARk MATter** (DAMA) collaboration has observed an annual modulation in their data [26] which is claimed to be due to dark matter particles in the galactic halo. Lately, some models have also been proposed to account for that modulation signal [27, 28].

On the other hand, indirect searches for WIMPs through their annihilation (or sometimes decay) into standard model degrees of freedom such as positrons, antiprotons or  $\gamma$  rays, which has been explored in several experiments [29, 30, 31, 32, 33] and neutrinos with experiments such as **Antarctic Muon And Neutrino Detector Array** (AMANDA) [34], **IceCUBE** [35], **Cubic Kilometer Size (KM3) Neutrino Telescope** (KM3NeT) [36]. Observations in the recent years such as the excess in the positron fraction reported by **High Energy Antimatter Telescope** (HEAT) [30], the **Payload of Antimatter Matter Exploration and Light-nuclei Astrophysics** (PAMELA) [31], **Advanced Thin Ionization Calorimeter** (ATIC) [32] and **Polar Patrol Balloon and Balloon borne Electron Telescope** with **Scintillating fibers** (PPB-BETS) [33], an excess in microwave emission around the galactic center [37] (also called the “WMAP Haze”), a bright 511 keV gamma-ray line from the Galactic Center region from

**INTE**rnational **G**amma **R**ay **A**strophysics **L**aboratory (INTEGRAL) [38], and an excess in the flux of 1-10 GeV diffuse galactic  $\gamma$  rays from **E**nergetic **G**amma **R**ay **E**xperiment **T**elescope (EGRET) data [39] have made researchers more excited in their quest for dark matter. Theoretical studies of the indirect dark matter detection via neutrino signals has recently received a lot of attention [40, 41].

In this paper, our focus is on the muon energy distributions from  $\nu_\mu + \bar{\nu}_\mu$  in neutrino telescopes due to annihilation of WIMPs which are captured in the core of the Earth (or the Sun) via gravitational interaction, or from annihilation of relic neutrinos [42]. As a result of these annihilations, neutrinos are produced at energies of the order of the mass of the WIMP and they interact on their way to the detector producing an observable muon flux. There is an extensive literature on WIMP annihilation in the Earth's or Sun's core [7, 15, 21, 22]. Here, we present a systematic way of calculating this muon flux for a few choices of annihilation channel. Our results can be used to determine the muon flux as a function of energy for a specific dark matter model by summing all the contributions from each annihilation mode weighted with corresponding branching fractions. We also compare our muon energy distributions with those obtained using other theoretical frameworks widely used in the literature [10, 11, 21, 22, 41].

The muon neutrino flux from weakly interacting dark matter annihilation ( $\chi\chi$  annihilation) depends on the dark matter capture rate and the dark matter annihilation rate. In the next section, we review the standard evaluation of the (muon) neutrino flux. This is followed by a discussion of the theoretical framework of muon survival probabilities and the resulting muon flux. Results are shown in Section IV, followed by our conclusions in Section V. The Appendix includes details of the muon neutrino energy distribution from various decay modes of fermions  $F$  in  $\chi\chi \rightarrow F\bar{F}$  where  $F = \nu, \tau, c$  and  $b$ .

## II. NEUTRINO FLUX FROM DARK MATTER ANNIHILATION

The dark matter particles can be captured in the core of the Sun or the Earth by interacting with the nuclei in the medium. This results in a WIMP density in the core that is considerably higher than in the galactic halo. The capture rate ( $C$ ) depends on the composition of the medium, the WIMP-nucleus interaction cross sections ( $\sigma_0^i$ ), the WIMP mass ( $m_\chi$ ), the local dark matter density ( $\rho^\chi$ ) and velocity ( $\bar{v}$ ) distribution of the WIMPs in the halo. After being accumulated in the core of these dense objects, the WIMPs annihilate with rate  $\Gamma_A$  into standard model particles which may further decay into neutrinos. These neutrinos can reach Earth-based detectors and create fluxes of charged leptons as a consequence of neutrino charged-current (CC) interactions.

The resulting fluxes depend on how the capture and

annihilation processes have occurred initially, however, in equilibrium these two processes are related: for every two WIMPs captured, one annihilation takes place so  $\Gamma_A = C/2$ . This equilibrium condition leads to a maximal flux which depends on the capture rate given by [7, 16, 17],

$$C = c \frac{\rho_{0.3}^\chi}{(m_\chi/\text{GeV})\bar{v}_{270}} \sum_i F_i(m_\chi) f_i \phi_i S(m_\chi/m_{N_i}) \times \frac{\sigma_0^i}{10^{-8} \text{ pb}} \frac{1 \text{ GeV}}{m_{N_i}}, \quad (1)$$

where

$$\rho_{0.3}^\chi = \frac{\rho^\chi}{0.3 \text{ GeV/cm}^3}, \quad \bar{v}_{270} = \frac{\bar{v}}{270 \text{ km/s}} \quad (2)$$

and

$$c = \begin{cases} 4.8 \times 10^{11} \text{s}^{-1} & \text{Earth,} \\ 4.8 \times 10^{20} \text{s}^{-1} & \text{Sun.} \end{cases} \quad (3)$$

The summation in Eq. (1) is over all species of nuclei in the astrophysical object,  $m_{N_i}$  is the mass of the  $i$ th nuclear species with mass fraction  $f_i$  relative to the Sun (or the Earth). The kinematic suppression factor, denoted by  $S(m_\chi/m_{N_i})$ , for a capture of WIMP of mass  $m_\chi$  from a nucleus of mass  $m_{N_i}$  is given by [7, 16, 17]

$$S(x) = \left( \frac{A^{1.5}}{1 + A^{1.5}} \right)^{\frac{2}{3}} \quad (4)$$

where

$$A(x) = \frac{3}{2} \frac{x}{(x-1)^2} \left( \frac{\langle v_{esc} \rangle}{\bar{v}} \right)^2. \quad (5)$$

For the Sun,  $\langle v_{esc} \rangle = 1156 \text{ km/s}$  and for the Earth,  $\langle v_{esc} \rangle = 13.2 \text{ km/s}$ . We also note that  $S(x) \rightarrow 1$  for  $x \rightarrow 1$ , which means that the capture process is kinematically suppressed if  $m_\chi$  differs from  $m_{N_i}$ , and there is no suppression if these masses are the same.

The other quantities in the capture rate expression are the form factor suppression  $F_i(m_\chi)$  and the velocity distribution function  $\phi_i$  of the  $i$ th element. The former one is due to the finite size of the nucleus which disrupts the coherence in the scattering process, thus, the form factor suppression is a negligible effect for capture from scattering with hydrogen and helium whereas it becomes important for larger nuclei. The velocity distribution function  $\phi_i$  depends on the velocity distribution squared of the element averaged over the volume of the astrophysical object ( $\langle v_i^2 \rangle$ ) and is given as [7, 16, 17],

$$\phi_i = \frac{\langle v_i^2 \rangle}{\langle v_{esc}^2 \rangle}. \quad (6)$$

If the massive astrophysical object is far from equilibrium, which is most likely the case for the Earth, the

annihilation rate is not only dependent on the capture rate but also on the annihilation cross section ( $\sigma$ ) via,

$$\Gamma_A = \frac{C}{2} \tanh^2(t_0 \sqrt{CC_A}) \quad (7)$$

where

$$C_A = \frac{\langle \sigma v \rangle}{V_{\text{eff}}} \quad (8)$$

and  $V_{\text{eff}}$  is the effective volume of the core of the Earth or Sun, while  $t_0$  is the age of the solar system. It is obvious from this relation that the equilibrium condition holds only when  $t_0 \sqrt{CC_A} \gg 1$ .

The flux of neutrinos of flavor  $i$  from dark matter annihilation into standard model particles can be written as

$$\left( \frac{d\phi_\nu}{dE_\nu} \right)_i = \frac{\Gamma_A}{4\pi R^2} \sum_F B_F \left( \frac{dN_\nu}{dE_\nu} \right)_{F,i}, \quad (9)$$

where  $(dN_\nu/dE_\nu)_{F,i}$  is the differential energy spectrum of neutrino flavor  $i$  from production of particles in channel  $F$ . In general, this energy spectrum is a function of the neutrino energy  $E_\nu$  and the energy of the produced particle,  $E_{in}$ . The differential neutrino energy spectra from a few dark matter annihilation channels are given in the Appendix. The quantity  $R$  is the Sun-Earth distance for neutrinos produced in the core of the Sun, or the radius of the Earth for the neutrinos created in the core of the Earth. The sum in Eq. (9) is over all annihilation channels  $F$  weighted with corresponding branching fractions  $B_F$ .

Neutrinos can be detected via their charged current interactions near or in the detector. To avoid the downward muon background, upward events where neutrinos interact with the nucleons in the rock below the detector producing muons which then travel up through the detector are one category of events. The other are contained events, in which the muon neutrinos produce muons in the detector ice. In the following sections, we focus on evaluating muon energy distribution from interactions of the neutrinos produced in the annihilation of the dark matter in the core of the Earth, in the core of the Sun and cosmic diffuse neutrinos from dark matter annihilation in the halos.

### III. MUON FLUX

The muon flux from muon neutrinos from DM annihilation depends on the flux of muon neutrinos as calculated with Eq. (9) and attenuation, tau neutrino regeneration and neutrino mixing in transit to the detector. For the energies of interest, neutrino mixing for DM annihilation in the Earth's core is not important. For annihilations in the Sun, neutrino mixing and tau neutrino regeneration may affect the flux of muon neutrinos when

$m_\chi$  is large. We neglect these effects because we consider the value of  $m_\chi$  for which only moderate modification of the muon neutrino flux is expected [10].

For upward events where the muon is produced outside the detector, muon energy loss is important. The most straightforward evaluation is for contained events, so we start with this case.

In the sections below, we focus on the neutrino induced flux of muons, produced either in the detector or near the detector with muon energy loss included. The detector may be modeled by an effective area. For Ice-Cube, an effective area for muons,  $A_{\text{eff}}(E_\mu, \theta)$ , can be simply parameterized as a function of the muon energy at the detector [43].

#### A. Contained Events

Contained events involve neutrino conversions within the detector volume. Denote the muon neutrino flux from a source of DM annihilations in the Earth's core or the Sun's core at location  $R$  from what is effectively a point source by

$$\frac{d\phi_\nu}{dE_\nu}(E_\nu, R).$$

The probability of the conversion of a neutrino with energy  $E_\nu$  into a muon with energy  $E_\mu$  over a distance  $dr$  through CC interactions is given by

$$dP_{CC} = dr dE_\mu \left( \rho_p \frac{d\sigma_\nu^p(E_\nu, E_\mu)}{dE_\mu} + (p \rightarrow n) \right). \quad (10)$$

Here,  $\rho_p$  and  $\rho_n$  are the number densities of protons and neutrons in the medium, respectively. We assume that  $\rho_p = \rho_n = \frac{1}{2} N_A \rho$  where  $N_A \simeq 6 \times 10^{23}$  is Avogadro's number. The differential cross sections  $d\sigma_\nu^{p,n}/dE_\mu$  are the weak scattering cross sections of (anti-)neutrinos on nucleus, which can be approximated by [10]

$$\frac{d\sigma_\nu^{p,n}}{dE_\mu} = \frac{2m_p G_F^2}{\pi} \left( a_\nu^{p,n} + b_\nu^{p,n} \frac{E_\mu^2}{E_\nu^2} \right) \quad (11)$$

with  $a_\nu^{n,p} = 0.25, 0.15$ ,  $b_\nu^{n,p} = 0.06, 0.04$  and  $a_{\bar{\nu}}^{n,p} = b_\nu^{p,n}$ ,  $b_{\bar{\nu}}^{n,p} = a_\nu^{p,n}$ . The contained event rate, for a detector with size  $\ell$ , is

$$\begin{aligned} \frac{d\phi_\mu}{dE_\mu} &= \int_R^{R+\ell} dr \int_{E_\mu}^{m_\chi} dE_\nu \frac{dP_{CC}}{dr dE_\mu} \frac{d\phi_\nu}{dE_\nu}(E_\nu, R) \\ &+ (\nu \rightarrow \bar{\nu}) \end{aligned} \quad (12)$$

where the neutrino flux is essentially independent of position in the detector given the scale of the Earth.

The neutrino flux from DM annihilation in the Earth's core is not attenuated, to a good approximation, until the neutrino interaction length approaches the radius of the Earth. This occurs at a neutrino energy of approximately

100 TeV. The neutrino flux in Eq. (12) is given by Eq. (9), with  $R \equiv R_E \simeq 6400$  km, the radius of the Earth, i.e.

$$\frac{d\phi_\nu}{dE_\nu}(E_\nu, R_E) = \frac{\Gamma_A}{4\pi R_E^2} \sum_F B_F \left( \frac{dN_\nu}{dE_\nu} \right)_{F,\mu}. \quad (13)$$

The density of the Sun is such that one needs to take into account neutrino attenuation due to its charged-current interactions as they pass through the Sun. In our calculations, we approximate attenuation with the exponential decrease in the flux over a distance  $\delta r'$  in the Sun, assuming that the composition of the Sun is mostly elemental hydrogen which has mass  $m_H = 0.931$  GeV.

$$\frac{d\phi_\nu}{dE_\nu}(r' + \delta r') = \exp(-\rho(r')\sigma_{CC}\delta r'/m_H) \frac{d\phi_\nu}{dE_\nu}(r') \quad (14)$$

where the neutrino flux  $d\phi_\nu(r')/dE_\nu$  is given by Eq. (12) with  $R_E$  being replaced by the distance from the Sun to the Earth,  $R_{SE}$ . We use the Sun density profile given by [44]

$$\rho(r') = 236.93 \text{ g/cm}^3 \times \exp(-10.098 \frac{r'}{R_S}), \quad (15)$$

where  $R_S$  is the radius of the Sun and we sum up all  $\delta r'$  contributions until neutrinos reach the surface of the Sun.

## B. Upward Events and Muon Energy Loss

High energy muons produced in neutrino charged-current interactions lose energy before they reach the detector as they travel through the rock or ice. The average energy loss of the muons with energy  $E$  over a distance  $dz$  during their passage through a medium with density  $\rho$  is given by,

$$\left\langle \frac{dE}{dz} \right\rangle = -(\alpha + \beta E)\rho, \quad (16)$$

where,  $\alpha \simeq 2 \times 10^{-3}$  GeV cm<sup>2</sup>/g accounts for the ionization energy loss and  $\beta \simeq 3.0 \times 10^{-6}$  cm<sup>2</sup>/g accounts for the bremsstrahlung, pair production and photonuclear interactions. The parameter  $\alpha$  is relatively insensitive to the composition of the material. The quantity  $\beta$  depends on composition of the medium and varies slowly with energy [45, 46, 47], and the average energy loss formula is not strictly applicable because of stochastic energy losses [47, 48]. For our purposes here, given the other uncertainties, using a constant  $\beta$  and approximating

$$\frac{dE}{dz} \simeq \left\langle \frac{dE}{dz} \right\rangle \quad (17)$$

is sufficient.

With this assumption the initial energy at  $z = 0$ ,  $E_\mu^i$ , is related to the final energy  $E_\mu^f$  after traveling a distance  $z$  by

$$E_\mu^i(z) = e^{\beta\rho z} E_\mu^f + (e^{\beta\rho z} - 1) \frac{\alpha}{\beta}. \quad (18)$$

At low energies, for  $E_\mu \leq 200$  GeV, the contribution from  $\beta$  term is small (about 10–20%) and in this energy range,

$$E_\mu^i(z) \simeq E_\mu^f + \alpha\rho z. \quad (19)$$

Muons with energies of a few 100 GeV are stopped in the rock ( $\rho \simeq 2.6$  g/cm<sup>3</sup>) before they decay. As an example, the stopping distance for 500 GeV muons is roughly 1 km whereas the decay length,  $\gamma c\tau$ , for these muons turns out to be about 3000 km. For 50 GeV muons, the decay length is about 300 km, compared to a stopping distance of 100 m.

The decay length information can still be included in the calculation by introducing the survival probability as the solution to the equation,

$$\frac{dP_{\text{surv}}}{dE_\mu} = \frac{P_{\text{surv}}}{E_\mu c\tau\rho(\alpha + \beta E_\mu)/m_\mu}. \quad (20)$$

This leads us to the survival probability for a muon with initial energy  $E_\mu^i$  and final energy  $E_\mu^f$ ,

$$P_{\text{surv}}(E_\mu^i, E_\mu^f) = \left( \frac{E_\mu^f}{E_\mu^i} \right)^\Gamma \left( \frac{\alpha + \beta E_\mu^i}{\alpha + \beta E_\mu^f} \right)^\Gamma \quad (21)$$

where  $\Gamma \equiv m_\mu/(c\tau\alpha\rho)$ .

With a distinction made between the energy of the muon when it is produced and the energy of the muon when it arrives at the detector for upward events, the formula for the upward muon flux is more complicated than Eq. (12). Instead, we have

$$\begin{aligned} \frac{d\phi_\mu}{dE_\mu} &= \int_{R_{\text{min}}}^R dr \int_{E_\nu^{\text{min}}}^{m_\times} dE_\nu \frac{dP_{CC}}{dr dE_\mu} \\ &\times \frac{d\phi_\nu}{dE_\nu} P_{\text{surv}}(E_\mu^i, E_\mu) \frac{dE_\mu^i}{dE_\mu} \\ &+ (\nu \rightarrow \bar{\nu}). \end{aligned} \quad (22)$$

where  $E_\mu \equiv E_\mu^f$ . The minimum neutrino energy in the integral is  $E_\nu^{\text{min}} = E_\mu^i(z)$ , where  $z = R - r$ . The maximum distance that muon travels to the detector and ends up with the final energy is  $R - R_{\text{min}}$  and the relationship between  $E_\mu$  and  $E_\mu^i$  given by Eq. (16).

Consider as a specific example annihilation at the core of the Earth. The detector is at a distance  $R = R_E \simeq 6400$  km from the core. In principle,  $R_{\text{min}} = 0$ , however, only muons produced near the detector will have sufficient energies to make it to the detector with an energy above the detector threshold energy  $E_{\text{th}}$ . The muon average range is

$$R_\mu(E_\mu^i, E_{\text{th}}) = \frac{1}{\beta\rho} \ln \left( \frac{\alpha + \beta E_\mu^i}{\alpha + \beta E_{\text{th}}} \right) \quad (23)$$

following from Eq. (18). For an initial muon energy of 1 TeV, the muon average range is 1 km for a muon threshold energy of 50 GeV. In practice, then,  $R_{min} = R_E - \Delta$ , where  $\Delta$  is, in general, less than 1 kilometer for the energies considered here. The upper limit for muon range is obtained by setting  $E_\mu^i = m_\chi$ , in which case  $\Delta = R_\mu(m_\chi, E_\mu)$ .

A change of variable from  $r$  to  $z = R_E - r$  yields a more familiar form of the integral for the muon flux from DM annihilations in the Earth's core,

$$\begin{aligned} \frac{d\phi_\mu}{dE_\mu} &= \frac{\Gamma_A}{4\pi R_E^2} \int_0^{R_\mu(m_\chi, E_\mu)} dz e^{\beta\rho z} \int_{E_\mu^i}^{m_\chi} dE_\nu \left( \frac{dN_\nu}{dE_\nu} \right)_{F,\mu} \\ &\times \left( \frac{E_\mu}{E_\mu^i} \frac{\alpha + \beta E_\mu^i}{\alpha + \beta E_\mu} \right)^\Gamma \times \left\{ \frac{d\sigma_\nu^p}{dE_\mu^i} \rho_p + (p \rightarrow n) \right\} \\ &+ (\nu \rightarrow \bar{\nu}). \end{aligned} \quad (24)$$

Throughout Eq. (24), the initial muon energy is implicitly a function of the final muon energy and the distance traveled,  $E_\mu^i = E_\mu^i(E_\mu, z)$  from Eq. (18).

Muon flux from DM annihilation in the Sun is given by

$$\begin{aligned} \frac{d\phi_\mu}{dE_\mu} &= \frac{\Gamma_A}{4\pi R_{SE}^2} \int_0^{R_\mu(m_\chi, E_\mu)} dz e^{\beta\rho z} \int_{E_\mu^i}^{m_\chi} dE_\nu \left( \frac{dN_\nu}{dE_\nu} \right)_{F,\mu} \\ &\times \left( \frac{E_\mu}{E_\mu^i} \frac{\alpha + \beta E_\mu^i}{\alpha + \beta E_\mu} \right)^\Gamma \times \left\{ \frac{d\sigma_\nu^p}{dE_\mu^i} \rho_p + (p \rightarrow n) \right\} \\ &\times \prod_{\delta r'} \exp(-\rho(r') \sigma_{CC} \delta r' / m_H) \frac{d\phi_\nu}{dE_\nu}(r') \\ &+ (\nu \rightarrow \bar{\nu}). \end{aligned} \quad (25)$$

## IV. RESULTS

### A. DM annihilation in the Earth's core

To illustrate the muon flux's dependence on muon energy, we begin with DM annihilation in the Earth's core. In addition to making a choice for  $m_\chi$ , one must also make some assumptions about the cross section and main channel to produce neutrinos. For all of the figures for DM annihilation, we use  $\sigma_0^i \simeq 10^{-8} N_i^4$  pb [21] and the standard composition of the Earth as reviewed in Ref. [7].

The upper curves in Fig. 1 show our results for  $\chi\chi \rightarrow \nu_\mu \bar{\nu}_\mu$  with  $B_{\nu_\mu} = 1$ , for upward events (dot-dashed curve) and contained events (dashed curve) for  $m_\chi = 500$  GeV. The lower dot-dot-dashed and dot-dash-dashed curves in Fig. 1 come from  $\chi\chi \rightarrow \tau^+ \tau^-$  with  $B_\tau = 1$ , followed by  $\tau \rightarrow \nu_\tau \mu \bar{\nu}_\mu$  according to the energy distribution in the Appendix. We choose the tau channel as representative of the three body decays that also occurs in heavy flavor semileptonic decays.

For direct production of neutrinos,  $d\phi_\nu/dE_\nu \propto \delta(m_\chi - E_\nu)$ . The cross section for neutrino production of muons smears the distribution. For contained events, one sees the smeared distribution directly in Fig. 1. Upward events have the additional energy redistribution from muon energy loss in transit that shifts the muon energy distribution to lower energies, enhancing the lower energy flux relative to the contained flux, despite the fact that the range is shorter than  $\ell = 1$  km. In the cascade of  $\tau \rightarrow \nu_\mu \rightarrow \mu$ , shown with the lower curves, there is never a high energy peak and the upward events are always below the contained events for this value of  $m_\chi$ . Only for  $m_\chi$  sufficiently higher than 1 TeV could the upward events be enhanced relative to the contained events.

As an indication of the atmospheric neutrino background, we also show upward (solid curve) and contained events (dotted curve) from a solid angle defined by a cone of half-angle  $1^\circ$  around the upward vertical direction. We use a simple parametrization for the flux of atmospheric  $\nu_\mu + \bar{\nu}_\mu$  (in units of  $\text{GeV}^{-1} \text{km}^{-2} \text{yr}^{-1} \text{sr}^{-1}$ ) from Ref. [49],

$$\begin{aligned} \frac{d\phi_\nu}{dE_\nu d\Omega} &= N_0 E_\nu^{-\gamma-1} \\ &\times \left( \frac{a}{1 + b E_\nu \cos\theta} + \frac{c}{1 + e E_\nu \cos\theta} \right). \end{aligned} \quad (26)$$

where the values of the parameters  $N_0$ ,  $\gamma$ ,  $a$ ,  $b$ ,  $c$  and  $e$  are given in Table 1. The approximate angular resolution of the IceCube detector is  $\theta = 1^\circ$ , however, DM annihilation can occur at angles larger than  $1^\circ$ . In particular, for a 500 GeV neutralino, it has been shown [22] that most of the annihilation occurs within an angle of  $\theta \sim 2.7^\circ$ . With this larger nadir angle, the solid angle for the atmospheric background is increased by a factor of  $\sim 8$ .

The shape of the background atmospheric flux is very different from the signal of contained events for direct annihilation of DM into neutrinos. With the atmospheric contained events in the figure multiplied by a factor of 8, the contained event rate would dominate the background only for the high energy peak. Our sample calculation is for  $B_\nu \sigma_0^i = 10^{-8} N_i^4$  pb $^{-1}$ , in which the capture and annihilation rates are in equilibrium. For the secondary neutrino production, from  $\tau$  decay, one needs  $B_\tau \sigma_0^0 \sim 10^{-7} N_i^4$  pb $^{-1}$  for this channel to be comparable to the background. Clearly measurements of the shape of the muon flux, both contained and upward, would be useful in searching for the dark matter signal.

These values of the cross section  $\sigma_0^i$  required for signals on the order of the atmospheric background are sufficient for the condition for the equilibrium between capture and annihilation in the Earth's core to be satisfied. Even though only with significant enhancements of the capture rate (i.e. WIMP-nucleon cross section) or DM annihilation rate, the Earth might be a source of measurable rates for DM annihilation to neutrinos, it is a useful demonstration of the energy dependence of the muon flux.

The energy dependence of Fig. 1 is at odds with the muon energy dependence sometimes found in the litera-

|          |   |
|----------|---|
| $\gamma$ | 1.74                                    |
| $a$      | 0.018                                   |
| $b$      | $0.024 \text{ GeV}^{-1}$                |
| $c$      | 0.0069                                  |
| $e$      | $0.00139 \text{ GeV}^{-1}$              |
| $N_0$    | $1.95 \times 10^{17}$ for $\nu$         |
|          | $1.35 \times 10^{17}$ for $\bar{\nu}$ . |

TABLE I: Parameters for the atmospheric  $\nu_\mu + \bar{\nu}_\mu$  flux, in units of  $\text{GeV}^{-1}\text{km}^{-2}\text{yr}^{-1}\text{sr}^{-1}$ .

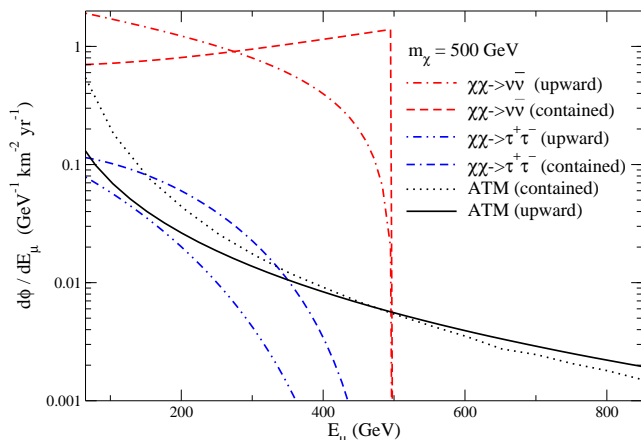


FIG. 1: Muon flux obtained from dark matter annihilation into neutrinos in the core of the Earth, when muons are created in neutrino interactions with nucleons in the rock below the detector (dot-dashed and dot-dot-dashed curves), when muons are created in the detector, i.e. contained events (dashed and dot-dash-dashed curves). The upper curves are for the direct production of neutrinos, while the lower curves are for neutrinos from tau decays. The background from contained atmospheric neutrinos, evaluated for a cone of angle  $\theta = 1^\circ$  are shown with the dotted (black) curve and the upward muon flux from atmospheric neutrinos is shown by the solid (black) curve.

ture [10, 11, 21, 41]. There, the upward flux of muons is written as

$$\frac{d\phi_\mu}{dE_\mu} = \frac{\Gamma_A}{4\pi R_E^2} \int_{E_\mu}^{m_\chi} dE_\nu \left( \frac{dN_\nu}{dE_\nu} \right)_{F,\mu} R_\mu(E_\mu, E_{th}) \times \left\{ \frac{d\sigma_\nu^p}{dE_\mu} \rho_p + (p \rightarrow n) \right\} + (\nu \rightarrow \bar{\nu}), \quad (27)$$

where  $E_{th} = 50 \text{ GeV}$ . This expression accounts for the fact that muons have a range with an energy dependence, however, it does not account for the fact that over the distance  $R(E_\mu, E_{th})$ , the muon has a final energy of  $E_{th}$ . Eq. (27) does not represent the energy dependent muon

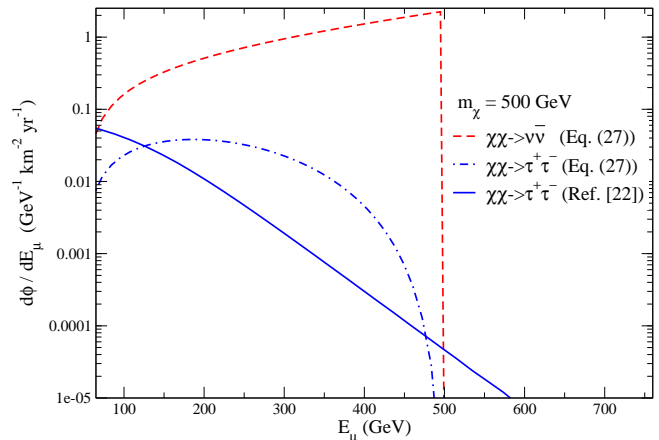


FIG. 2: Upward muons flux obtained using Eq. (27) for  $\chi\chi \rightarrow \nu_\mu \bar{\nu}_\mu$  (dashed curve) and for  $\chi\chi \rightarrow \tau^+ \tau^-$ , followed by  $\tau \rightarrow \nu_\tau \mu \bar{\nu}_\mu$  (dot-dashed curve), and the muon upward flux for  $\chi\chi \rightarrow \tau^+ \tau^-$  channel from Ref. [22] (solid curve). The upward muon flux from Eq. (27) is inconsistent with the upward flux shown in Fig. 1.

flux, however, the integral number of upward events with  $E_\mu > E_{th}$  obtained using Eq. (27) and the results using Eq. (22) are approximately equal. In Fig. 2, we show the upward muon fluxes from Eq. (27), for the direct neutrino production (dashed curve) and from the  $\tau$  decay (dot-dashed curve). Comparing results from Figs. 1 and 2, we find that the upward muon flux of Eq. (27) for  $\chi\chi \rightarrow \nu\bar{\nu}$  case follows more closely the contained muon flux at high energies presented in Fig.1 (dashed curve) than the upward flux, with an enhancement at high  $E_\mu$  because the muon range increases with muon energy. Clearly, the upward muon flux in Fig. 2 (dashed curve) does not accurately reflect the muon energy distribution of upward events from DM annihilation in the Earth. Similarly, a comparison of upward muon flux for  $\chi\chi \rightarrow \tau^+ \tau^-$ , followed by  $\tau \rightarrow \nu_\tau \mu \bar{\nu}_\mu$ , obtained using Eq. (27) has a very different shape than the same flux obtained with Eq. (23). Comparable discrepancies are found between upward fluxes from Eq. (27) and our evaluation of upward events for DM annihilation in the Sun as well.

We also show with the solid line in Fig. 2 the results for upward muon flux from the  $\chi\chi \rightarrow \tau^+ \tau^-$  from Ref. [22]. In Ref. [22], the flux of muons comes from a PYTHIA simulation of the resultant muon neutrino flux and a simulation of muon electromagnetic energy loss. A dark matter distribution has been assumed in the Earth's core and contribution from dark matter annihilation around the center of the core with specific angular cuts ( $\theta \leq 5^\circ$ ) have been applied, so the normalization

should be lower. The energy distribution has qualitatively the same behavior as our results, however, it does not vanish at the kinematic limit when  $E_\mu = m_\chi$ .

## B. DM annihilation in the Sun

Similar conclusions can be derived in the case of capture of WIMPs in the core of the Sun. As noted earlier, there is attenuation of the initial neutrino flux as it propagates from the core to the exterior of the Sun. The interaction length of the neutrinos with energy  $\sim 30$  GeV becomes equal to the column depth of the Sun (the average density of the core of the Sun is  $\sim 150$  g/cm<sup>3</sup>). At higher energies, the interaction length becomes even smaller and the neutrino flux is reduced significantly. We do not include neutrino oscillation in the Sun [10], which depending on the dark matter model, might affect the flux of  $\nu_\mu + \bar{\nu}_\mu$ .

In Fig. 3, we show the upward muon and the contained muon fluxes for the direct production and for the  $\tau$  production channels. In our calculations, we approximate neutrino attenuation in the Sun with an exponential suppression as presented in the previous section. We note that this effect becomes stronger for higher neutrino energies which manifests itself when  $m_\chi$  is large. Recall that the charged current neutrino nucleon cross section increases with the neutrino energy. As an example, the muon flux decreases by a factor of 3 for  $m_\chi = 250$  GeV, factor of 10 for  $m_\chi = 500$  GeV and two orders of magnitude for  $m_\chi = 1$  TeV, as compared to the case with no attenuation.

We compare our results for muon flux with those in Ref. [22], where there is assumption of dark matter distribution in the core of the Sun and contribution from dark matter annihilation around the center of the core with specific angular cuts have been applied. Effects due to neutrino flavor oscillations in the Sun have not been incorporated. The shape of the energy distribution is similar to our result, but with lower normalization and with a lack of the kinematic cutoff when  $E_\mu = m_\chi$ .

As in the case of the Earth, the upward muon flux from  $\chi\chi \rightarrow \nu\bar{\nu}$  is larger than the contained flux for muon energies,  $E_\mu < 380$  GeV, while in the case when neutrinos are produced via  $\chi\chi \rightarrow \tau^+\tau^-$ , followed by  $\tau \rightarrow \nu_\tau\mu\bar{\nu}_\mu$ , the contained muon flux is always larger than the upward flux. We also show the angle-averaged atmospheric flux for a cone of half-angle  $1^\circ$ . For direct annihilation into neutrinos for the model in which the branching fraction is of the order of one, the signal is larger than the atmospheric background for both contained and upward muons. For the tau channel, signal is comparable to the background for upward muons when muons have energy around 200 GeV, however taking into account the effects of kinematics on the angular pointing of the muons at low energy may make this less apparent.

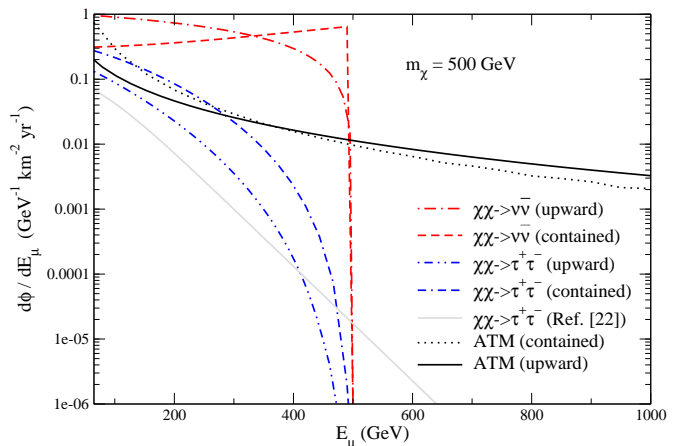


FIG. 3: Muon fluxes obtained from dark matter annihilation into neutrinos in the core of the Sun, for upward events (dot-dashed and dot-dot-dashed curves), and for contained events (dashed and dot-dash-dashed curves). The upper curves are for the direct production of neutrinos, while the lower curves are for neutrinos from tau decays. Background upward muons are shown with the solid (black) curve and the contained muons are shown with the dotted (black) curve, where the evaluation used the angle-averaged atmospheric neutrino flux integrated over a solid angle with  $\theta = 1^\circ$ . The grey solid curve is from Edsjö's parameterization of the muon flux [22].

## C. Muons in IceCube

With the upward muon fluxes evaluated above from annihilation of DM in the Earth and the Sun, it is possible to estimate the event rate of muons in IceCube using the muon effective area [43]. Following Ref. [43], we parameterized

$$A_{eff}(E_\mu, \theta) \simeq 2\pi A_0(E_\mu)(0.92 - 0.45 \cos \theta) \quad (28)$$

where  $\theta$  is the zenith angle measured from vertical and

$$\begin{aligned} E_\mu &\leq 10^{1.6} \text{ GeV} : \\ A_0(E_\mu) &= 0 \\ 10^{1.6} \text{ GeV} &\leq E_\mu \leq 10^{2.8} \text{ GeV} : \\ A_0(E_\mu) &= 0.748(\log_{10}(E_\mu/\text{GeV}) - 1.6) \text{ km} \\ 10^{2.8} \text{ GeV} &\leq E_\mu : \\ A_0(E_\mu) &= 0.9 + 0.54(\log_{10}(E_\mu/\text{GeV}) - 2.8) \text{ km} . \end{aligned}$$

This effective muon area models the threshold detection effects near  $E_\mu \sim 50$  GeV and local rock and ice below the IceCube detector [43].

To facilitate comparisons with other muon energy dis-



tributions which appear in the literature, we evaluate

$$\frac{dN_\mu}{dE_\mu} = \frac{d\phi_\mu}{dE_\mu} \cdot \langle A_{eff}(E_\mu, \theta) \rangle \quad (29)$$

for DM annihilation to neutrinos in the Earth and Sun which convert to muons outside the detector. Here,  $\langle A_{eff} \rangle$  is the angle averaged effective area, averaged over zenith angles  $\theta = \pi/2 - \pi$ . Fig. 4 shows our results for the upward muon flux times effective area with the solid and dot-dashed lines (solid for the Earth), and by comparison, the results for the contained muon flux multiplied by  $1 \text{ km}^2$  (dotted and dashed lines, dotted for the Earth). The energy dependence of the effective area changes the shapes of the curves for upward muons at low energies, but it does not change the large discrepancies between our upward muon rates compared with Eq. (27) at energies closer to  $E_\mu \sim m_\chi$ .

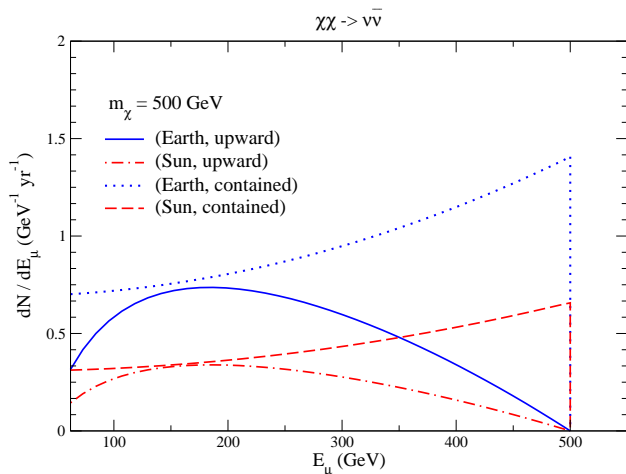


FIG. 4: The upward muon flux times muon effective area obtained from dark matter annihilation to neutrinos in the core of the Earth (solid line) and Sun (dot-dashed line). For comparison, we also show the contained muon flux times  $1 \text{ km}^2$  for the Earth (dotted) and for the Sun (dashed).

#### D. Cosmic Diffuse Neutrino Flux

In addition to the astrophysical object such as the Sun and the Earth being potential sources of dark matter, relic dark matter can also annihilate in halos in the universe [42], providing a promising source of cosmic diffuse neutrinos from dark matter annihilation.

To determine this flux one needs to sum over all halos to yield a flux of neutrinos. This diffuse neutrino flux depends on several factors such as the evolution with redshift, the radial density profiles and the number density

of halos of a given mass at a given redshift [42, 50, 51]. In Ref. [42], dark matter annihilation process,  $\chi\chi \rightarrow \nu\bar{\nu}$ , is proposed to be used to determine an upper limit on the annihilation cross section.

The cosmic diffuse neutrinos for the  $\chi\chi \rightarrow \nu\bar{\nu}$  channel from Ref. [42] is approximately a power law function of  $E_\nu$ , i.e.

$$\left( \frac{d\phi_\nu}{dE_\nu d\Omega} \right)_{\nu_\mu + \bar{\nu}_\mu} \simeq A \frac{(E_\nu/\text{GeV})^{0.5}}{(m_\chi/\text{GeV})^{3.5}} \quad E_\nu \leq m_\chi. \quad (30)$$

In Ref. [42], the normalization  $A$  is determined by setting the number of neutrinos from the diffuse flux (here approximated by Eq. (30)) equal to the number of atmospheric neutrinos from the same energy interval, from  $10^{-0.5} m_\chi$  to  $m_\chi$ , i.e.

$$\int_{\frac{m_\chi}{\sqrt{10}}}^{m_\chi} dE_\nu A \frac{(E_\nu/\text{GeV})^{0.5}}{(m_\chi/\text{GeV})^{3.5}} = \int_{\frac{m_\chi}{\sqrt{10}}}^{m_\chi} dE_\nu \left( \frac{d\phi_\nu}{dE_\nu d\Omega} \right)_{av} \quad (31)$$

where  $\left( \frac{d\phi_\nu}{dE_\nu d\Omega} \right)_{av}$  is the angle-averaged atmospheric flux given by Eq. (26). We consider here a case when  $m_\chi = 1 \text{ TeV}$ .

In Fig. 5, we show upward and contained muon fluxes from cosmic diffuse neutrinos, integrating over the full  $2\pi$  solid angle. For  $E_\mu > 400 \text{ GeV}$ , the contained flux dominates the upward flux, an artifact of the triangular shape of the neutrino flux. For comparison we also show the contained and upward fluxes for the atmospheric neutrino background. The falling energy spectrum of the atmospheric neutrinos results in the upward flux of muons from atmospheric neutrinos dominating the contained muon flux for  $E_\mu > 400 \text{ GeV}$  for  $m_\chi = 1 \text{ TeV}$ .

The direct production of neutrinos  $\chi\chi \rightarrow \nu\bar{\nu}$  is the most favorable channel in terms of neutrino detection for the diffuse DM limits since the muon flux stands out more from the background than the muons from a  $\chi \rightarrow \tau \rightarrow \nu_\mu$  cascade (or similar production and decay process). In addition, the  $\chi\chi \rightarrow \nu\bar{\nu}$  channel has no other astrophysical observable. Nevertheless, the muon flux is not as dramatic a peak in the falling neutrino induced atmospheric muon flux as the direct comparison of the neutrino fluxes is. A more comprehensive analysis of a diffuse DM annihilation signal could include both the  $\nu\bar{\nu}$  and cascade channels as possibilities, and focus on the muon signals rather than the neutrino signals.

#### V. CONCLUSIONS

We have calculated muon fluxes from dark matter annihilation, when dark matter is trapped in the the Sun's (Earth's) core and when dark matter annihilates in halos in the universe (cosmic diffuse flux). Without using a specific model for dark matter, we have considered  $\chi\chi \rightarrow \nu\bar{\nu}$  and  $\chi\chi \rightarrow \tau^+\tau^-$ , followed by  $\tau \rightarrow \nu_\tau \mu \bar{\nu}_\mu$  channels as representatives of direct and of the secondary neu-



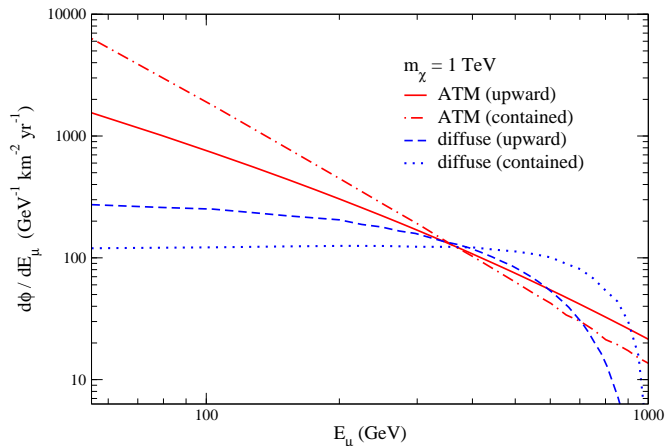


FIG. 5: Muon fluxes obtained from dark matter annihilation in the halos producing cosmic diffuse neutrinos: upward muons flux (dashed curve) and contained muon flux (dotted curve) compared with contained (dot-dashed curve) and upward (solid curve) muon fluxes from angle-averaged atmospheric neutrinos. Here, we take  $m_\chi = 1$  TeV.

trino production. We have taken into account neutrino attenuation as it propagates from the core of the Sun to its surface. In the evaluation of the upward muon flux, we have incorporated muon energy loss, as described by the muon range.

We have shown that our results exhibit a very different energy dependence than those obtained from Eq. (27) that is widely used in the literature [10, 21, 41], however, there is reasonably good agreement with the parameterization of Ref. [22] away from the region of maximum energy  $E_\mu \sim m_\chi$ . Our results are obtained with the assumption that the dark matter annihilation occurs at the maximum rate, when the annihilation rate is half the capture rate. This is reasonable for the Sun but requires significant enhancement of the capture rate (or annihilation cross section) for the Earth to be in equilibrium [21].

In our calculation we used spin independent WIMP-nucleon cross sections which have much stronger experimental bound than the spin dependent cross sections [52]. In the core of the Sun the capture rate might be dominated by the spin dependent (SD) WIMP-hydrogen nuclei interactions, which would increase the signal rates by a couple of orders of magnitude and still be consistent with Amanda limits on annihilation rates [53]. In the dark matter model in which there is a low velocity enhancement of the DM annihilation cross section [27], introduced as an explanation for the positron excess observed in cosmic ray experiments [30, 31, 32, 33], it is possible for the WIMPs in the core of the Earth to be in

the equilibrium as well.

Furthermore, incorporating neutrino oscillations and the regeneration effects in the Sun will likely affect the final muon flux especially in the models which possess an asymmetry in the initial neutrino fluxes or where  $\chi\chi \rightarrow \tau^+\tau^-$  is the dominant mode [10]. We have used a model independent normalization,  $\sigma_0^i \simeq 10^{-8} N_i^4$  pb and  $B_F = 1$  to evaluate the muon flux. We find that for this branching fraction signals from  $\chi\chi \rightarrow \nu\bar{\nu}$  and  $\chi\chi \rightarrow \tau^+\tau^-$ , followed by  $\tau \rightarrow \nu_\tau\mu\bar{\nu}_\mu$ , when DM annihilation happens in the core of the Sun, are comparable or even larger than the background (upward) muons from atmospheric neutrinos. In the case of direct neutrino production, the upward muon flux is larger than the contained flux for  $E_\mu < 350$  GeV for  $m_\chi = 500$  GeV, due to the muon range. When neutrinos are produced via secondary processes, contained events always dominate upward muons.

Cosmic diffuse neutrinos, produced directly in DM annihilation, give a very weak energy dependence of the contained and upward muon flux, in contrast to the steep energy dependence of the atmospheric background. The upward muon flux from cosmic diffuse neutrinos is dominant over the contained flux for muon energies below 400 GeV for  $m_\chi = 1$  TeV, which also happens to be the energy at which the signal becomes dominant over the background muons from atmospheric neutrinos.

Model dependence is an important element, for example,  $\chi\chi \rightarrow \nu\bar{\nu}$  is not allowed for DM at rest when the DM particles are neutralinos [10]. However, with the formalism developed, one can determine muon fluxes for specific dark matter model by summing up the contributions from all decay channels weighted with corresponding branching fractions [54]. Thus, measurements of the muon energy distribution in neutrino telescopes, such as IceCUBE and KM3, could provide valuable information about the origin of the dark matter sector and fundamental properties such as the dark matter mass and its couplings.

## Acknowledgments

M.H.R. and I.S. would like to thank Aspen Center for Physics for hospitality while this work was completed. We thank D. Marfatia and V. Barger for discussions. This research was supported by US Department of Energy contracts DE-FG02-91ER40664, DE-FG02-04ER41319 and DE-FG02-04ER41298.

## VI. APPENDIX: MUON NEUTRINO DISTRIBUTIONS

### A. Neutrino energy distribution from direct production:

Neutrino energy distribution when neutrinos are produced directly from dark matter annihilation is given by,

$$\frac{dN_\nu}{dE_\nu} = \delta(E_\nu - m_\chi) \quad (32)$$

### B. Neutrino energy distribution from $\tau^+\tau^-$ , $b\bar{b}$ , $c\bar{c}$ decay modes:

In these decay modes, we use the unpolarized decay distributions, so the  $\nu$  and  $\bar{\nu}$  distributions are assumed

to be the same. The decay branching fraction is denoted by  $B_f$  for a given decay mode  $f$ ,  $f = \nu, \tau, b, c$ . The  $b$  and  $c$  quarks hadronize before they decay into neutrinos. The hadronization effect is taken into account by scaling the initial quark energy,  $E_{in}$ , in the form  $E_d = z_f E_{in}$ , where  $z_f = 0.73, 0.58$  for  $b$  and  $c$  quarks, respectively [55].

Neutrino energy distribution from the decay of  $\tau^+\tau^-$ ,  $b\bar{b}$ ,  $c\bar{c}$  is approximately

$$\frac{dN_\nu}{dE_\nu} = \frac{2B_f}{E_{in}}(1 - 3x^2 + 2x^3), \quad \text{where } x = \frac{E_\nu}{E_{in}} \leq 1, \quad (33)$$

where

$$(E_{in}, B_f) = \begin{cases} (m_\chi, 0.18) & \tau \text{ decay,} \\ (0.73m_\chi, 0.103) & b \text{ decay,} \\ (0.58m_\chi, 0.13) & c \text{ decay.} \end{cases} \quad (34)$$

- 
- [1] See, e.g., L. Bergström, hep-ph/0903.4849 for a review.
- [2] A. Borriello and P. Salucci, *Mon. Not. Roy. Astron. Soc.* **323**, 285 (2001).
- [3] F. Zwicky, *Helv. Phys. Acta.* **6**, 110 (1933).
- [4] D.N. Spergel *et al.* [WMAP Collaboration], *Astrophys. J. Suppl.* **170**, 377 (2007).
- [5] E. Komatsu *et al.* [WMAP Collaboration], *Astrophys. J. Suppl. Ser.* **180**, 330 (2009).
- [6] M. Tegmark *et al.* [SDSS Collaboration], *Astrophys. J.* **606**, 702 (2004).
- [7] G. Jungman, M. Kamionkowski and K. Griest, *Phys. Rep.* **267**, 195 (1996).
- [8] F.D. Steffen, *Eur. Phys. J. C* **59**, 557 (2009).
- [9] See, for example, I.F.M. Albuquerque, L. Hui and E.W. Kolb, *Phys. Rev. D* **64**, 083504 (2001); P. Crotty, *Phys. Rev. D* **66**, 063504 (2002); F. Halzen and D. Hooper, *Nucl. Phys. Proc. Suppl.* **124**, 243 (2003).
- [10] V. Barger, W. Keung, G. Shaughnessy and A. Tregre, *Phys. Rev. D* **76**, 095008 (2007); V. D. Barger, F. Halzen, D. Hooper and C. Kao, *Phys. Rev. D* **65**, 075022 (2002).
- [11] D. Hooper and E.A. Baltz, *Ann. Rev. Nucl. Part. Sci.* **58**, 293 (2008).
- [12] G. 't Hooft, in *Proceedings of Nato Advanced Study Institute, Recent Developments In Gauge Theories*, edited by G. 't Hooft *et al.*, NATO Advanced Study Institutes, Ser. B Vol. **59**, (Plenum, New York, 1980), p. 135.
- [13] H. Baer and X. Tata, hep-ph/0805.1905.
- [14] See, e.g., G.B. Gelmini, *Int. J. Mod. Phys. A* **23**, 4273 (2008), and references therein.
- [15] M. Kamionkowski, *Phys. Rev. D* **44**, 3021 (1991); S. Ritz and D. Seckel, *Nucl. Phys. B* **304**, 877 (1988); W.H. Perez and D.N. Spergel, *Astrophys. J.* **296**, 679 (1985); J. Silk, K. Olive and M. Srednicki, *Phys. Rev. Lett.* **55**, 257 (1985); L.M. Krauss, K. Freese, D.N. Spergel and W.H. Press, *Astrophys. J.* **299**, 1001 (1985); K. Freese, *Phys. Lett. B* **167**, 295 (1986); L.M. Krauss, M. Srednicki and F. Wilczek, *Phys. Rev. D* **33**, 2079 (1986); T. Gaisser, G. Steigman and S. Tilav, *Phys. Rev. D* **34**, 2206 (1986).
- [16] G. Gelmini, P. Gondolo and E. Roulet, SISSA-88/89-EP (1989).
- [17] M. Kamionkowski, *Phys. Rev. D* **44**, 3021 (1991); A. Gould, *Astrophys. J.* **321**, 571 (1987).
- [18] J. Hisano, K. Nakayama and M.J.S. Yang, *Phys. Lett. B* **678**, 101 (2009); J. Liu, P. Yin and S. Zhu, *Phys. Rev. D* **79**, 063522 (2009); H. Yuksel, S. Horiuchi, J.F. Beacom and S. Ando, *Phys. Rev. D* **76**, 123506 (2007); G. Bertone, *Phys. Rev. D* **73**, 103519 (2006); G. Bertone, E. Nezri, J. Orloff and J. Silk, *Phys. Rev. D* **70**, 063503 (2004).
- [19] L. Bergstrom, J. Edsjö and P. Gondolo, *Phys. Rev. D* **58**, 103519 (1998); F. Halzen and J.E. Jacobsen, hep-ph/9406309; K. Ng, K.A. Olive and M. Srednicki, *Phys. Lett. B* **188**, 138 (1987); M. Srednicki, K.A. Olive and J. Silk, *Nucl. Phys. B* **279**, 804 (1987).
- [20] T. Bruch, A.H.G. Peter, J. Read, L. Baudis and G. Lake, *Phys. Lett. B* **674**, 250 (2009); M. Cirelli *et al.*, *Nucl. Phys. B* **727**, 99 (2005) [Erratum-ibid. **790**, 338 (2008)]; D. Elsaesser and K. Mannheim, *Astropart. Phys.* **22**, 65 (2004); D. Hooper and J. Silk, *New. J. Phys.* **6**, 23 (2004); R. Lehnert and T.J. Weiler, *Phys. Rev. D* **77**, 125004 (2008).
- [21] C. Delaunay, P.J. Fox and G. Perez, *JHEP* **0905**, 099 (2009).
- [22] J. Edsjö PhD thesis, Uppsala University, 1997; J. Edsjö, *Nucl. Phys. Proc. Suppl.* **43**, 265 (1995); G. Wikström and J. Edsjö, *J. Cosmol. Astropart. Phys.* **04** (2009)

- 009.
- [23] C.E. Aalseth *et al.* [IGEX Collaboration], Phys. Rev. C **59**, 2108 (1999); D. Gonzalez *et al.* [IGEX Collaboration], Nucl. Phys. Proc. Suppl. **87**, 278 (2000); H.V. Klapdor-Kleingrothaus and I.V. Krivosheina, Nucl. Phys. Proc. Suppl. **145**, 237 (2005); I.V. Krivosheina *et al.* [Heidelberg-Moscow and GENIUS Collaborations], Phys. Scripta T **127**, 52 (2006); G.J. Alner *et al.* [UK Dark Matter Collaboration], Phys. Lett. B **616**, 17 (2005); W.J. Bolte *et al.* [COUPP Collaboration], Nucl. Instrum. Meth. A **577**, 569 (2007); W.J. Bolte *et al.*, J. Phys. Conf. Ser. **39**, 126 (2006); A.V. Lubashevskiy *et al.* [EDELWEISS Collaboration], Phys. Atom. Nucl. **71**, 1298 (2008).
- [24] J. Angle *et al.* [XENON Collaboration], Phys. Rev. Lett. **100**, 021303 (2008).
- [25] Z. Ahmed *et al.* [CDMS Collaboration], Phys. Rev. Lett. **102**, 011301 (2009).
- [26] R. Bernabei *et al.* [DAMA Collaboration], Eur. Phys. J. C **56**, 333 (2008).
- [27] N. Arkani-Hamed, D.P. Finkbeiner, T.R. Slatyer and N. Weiner, Phys. Rev. D **79**, 015014 (2009).
- [28] See, for example, A. Bottino, F. Donato, N. Fornengo and S. Scopel, Phys. Rev. D **78**, 083520 (2008); S. Chang, A. Pierce and N. Weiner, Phys. Rev. D **79**, 115011 (2009); M. Fairbairn and T. Schwetz, JCAP **0901**, 037 (2009); D. Hooper, F. Petriello, K.M. Zurek and M. Kamionkowski, Phys. Rev. D **79**, 015010 (2009); C. Savage, G. Gelmini, P. Gondolo and K. Freese, JCAP **0904**, 010 (2009); S. Chang, G.D. Kribs, D. Tucker-Smit and N. Weiner, Phys. Rev. D **79**, 043513 (2009); R. Foot, Phys. Rev. D **78**, 043529 (2008); M.Y. Khlopov and C. Kouvaris, Phys. Rev. D **78**, 065040 (2008); J.L. Feng, J. Kumar and L.E. Strigari, Phys. Lett. B **670**, 37 (2008).
- [29] W.B. Atwood *et al.* [Fermi/LAT Collaboration], Astrophys. J. **697**, 1071 (2009); M. Aguilar *et al.* [AMS-01 Collaboration], Phys. Lett. B **646**, 145 (2007); C. Goy [AMS Collaboration], J. Phys. Conf. Ser. **39**, 185 (2006); D. Casadei, astro-ph/0609072; E.O. Wilhelm [HESS Collaboration], AIP Conf. Proc. **1112**, 16 (2009); M. Beilicke [VERITAS Collaboration], AIP Conf. Proc. **1112**, 33 (2009); T. Mizukami [CANGAROO-III Collaboration], AIP Conf. Proc. **1085**, 364 (2008); Y. Yukawa [CANGAROO Collaboration], J Phys. Conf. Ser. **120**, 062018 (2008); J. Rico *et al.* [MAGIC Collaboration], AIP Conf. Proc. **1112**, 23 (2009).
- [30] S.W. Barwick *et al.* [HEAT Collaboration], Astrophys. J. **482**, L191 (1997).
- [31] O. Adriani *et al.* [PAMELA Collaboration], Nature **458**, 607 (2009); E. Mocchiutti *et al.*, astro-ph.HE/0905.2551.
- [32] J. Chang *et al.*, Nature **456**, 362 (2008).
- [33] S. Torii *et al.* [PPB-BETS Collaboration], astro-ph/0809.0760; K. Yoshida *et al.*, Adv. Space Res. **42**, 1670 (2008).
- [34] J. Braun and D. Hubert [IceCube Collaboration], astro-ph.HE/0906.1615; D. Hubert [IceCube Collaboration], Nucl. Phys. Proc. Suppl. **173**, 87 (2007).
- [35] R. Abbasi *et al.* [IceCube Collaboration], Nucl. Instrum. Meth. A **601**, 294 (2009); C. Rott [IceCube Collaboration], astro-ph/0810.3698.
- [36] U.F. Katz [KM3NeT Collaboration], Nucl. Instrum. Methods Phys. Res., Sect. A **602**, 40 (2009).
- [37] D.P. Finkbeiner, Astrophys. J. **614**, 186 (2004); G. Dobler and D.P. Finkbeiner, Astrophys. J. **680**, 1222 (2008); M. Bottino, A.J. Banday and D. Maino, astro-ph/0807.1865; D. Hooper, D.P. Finkbeiner and G. Dobler, Phys. Rev. D **76**, 083012 (2007).
- [38] P. Jean *et al.*, Astron. Astrophys. **407**, L55 (2003); C. Boehm, D. Hooper, J. Silk, M. Casse and J. Paul, Phys. Rev. Lett. **92**, 101301 (2004).
- [39] S.D. Hunter *et al.*, Astrophys. J. **481**, 205 (1997); W. de Boer *et al.* astro-ph/0408272; W. de Boer, C. Sander, V. Zhukov, A.V. Gladyshev and D.I. Kazakov, Phys. Rev. Lett. **95**, 209001 (2005).
- [40] See, for example, P. Agrawal, E.M. Dolle and C.A. Krenke, Phys. Rev. D **79**, 015015 (2009); L. Covi, M. Grefe, A. Ibarra and D. Tran, JCAP **0901**, 029 (2009); S. Palomares-Ruiz and S. Pascoli, Phys. Rev. D **77**, 025025 (2008); D. Hooper and G.D. Kribs, Phys. Rev. D **67**, 055003 (2003); V. Bertin, E. Nezri and J. Orloff, Eur. Phys. J. C **26**, 111 (2002); J. Hisano, M. Kawasaki, K. Kohri and K. Nakayama, Phys. Rev. D **79**, 043516 (2009); G. Bertone, New Astron. Rev. **51**, 321 (2007); S. Andreas, T. Hambye and M. H. G. Tytgat, JCAP **0810**, 034 (2008); A. Kusenko and I. M. Shoemaker, Phys. Rev. D **80**, 027701 (2009).
- [41] A. Menon, R. Morris, A. Pierce and N. Weiner, hep-ph/0905.1847; D. Hooper, hep-ph/0901.4090; M. Beltran, D. Hooper, E.W. Kolb and Z.C. Krusberg, hep-ph/0808.3384; D. Hooper and G. Servant, Astropart. Phys. **24**, 231 (2005); G. Bertone, D. Hooper and J. Silk, Phys. Rept. **405**, 279 (2005); V.D. Barger, W.Y. Keung and G. Shaughnessy, Phys. Lett. B **664**, 190 (2008); F. Halzen and D. Hooper, Phys. Rev. D **73**, 123507 (2006) S. Nussinov, L. T. Wang and I. Yavin, arXiv:0905.1333 [hep-ph]; M. Blennow, J. Edsjo and T. Ohlsson, JCAP **0801**, 021 (2008).
- [42] J.F. Beacom, N.F. Bell and G.D. Mack, Phys. Rev. Lett. **99**, 231301 (2007); N.F. Bell, J.B. Dent, T.D. Jacques and T.J. Weiler, Phys. Rev. D **78**, 083540 (2008).
- [43] M. C. Gonzalez-Garcia, F. Halzen and S. Mohapatra, arXiv:0902.1176 [astro-ph.HE]; see also, M. C. Gonzalez-Garcia, F. Halzen and M. Maltoni, Phys. Rev. D **71**, 093010 (2005) [arXiv:hep-ph/0502223].
- [44] R. Gandhi, C. Quigg, M.H. Reno and I. Sarcevic, Astropart. Phys. **5**, 81 (1996).
- [45] D. Groom, N. Mokhov and S. Striganov, Atomic Data and Nuclear Data Tables **78**, 183 (2001).
- [46] S. Iyer Dutta, M. H. Reno, I. Sarcevic and D. Seckel, Phys. Rev. D **63**, 094020 (2001).
- [47] P. Lipari and T. Stanev, Phys. Rev. D **44**, 3543 (1991).
- [48] E. V. Bugaev, A. Misaki, V. A. Naumov, T. S. Sinogovskaya, S. I. Sinogovskiy and N. Takahashi, Phys. Rev. D **58**, 054001 (1998).
- [49] M. Honda, T. Kajita, K. Kasahara, S. Midorikawa and T. Sanuki, Phys. Rev. D **75**, 043006 (2007); T.K. Gaisser and M. Honda, Ann. Rev. Nucl. Part. Sci. **52**, 153 (2002).
- [50] P. Ullio, L. Bergstrom, J. Edsjo and C. Lacey, Phys. Rev. D **66**, 123502 (2002); L. Bergstrom, J. Edsjo and P. Ullio, Phys. Rev. Lett. **87**, 251301 (2001).
- [51] J.E. Taylor and J. Silk, MNRAS **339**, 505 (2003); K. Ahn and E. Komatsu, Phys. Rev. D **71**, 021303 (2005); S. Ando, Phys. Rev. Lett. **94**, 171303 (2005); S. Ando and E. Komatsu, Phys. Rev. D **73**, 023521 (2006).
- [52] J. Angle *et al.*, Phys. Rev. Lett. **101**, 091301 (2008); D.S. Akerib *et al.* [CDMS Collaboration], Phys. Rev. D

- 73**, 011102 (2006); G.J. Alner *et al.* [ZEPLIN-II Collaboration], Phys. Lett. B **653**, 161 (2007); H.S. Lee *et al.* [KIMS Collaboration], Phys. Rev. Lett. **99**, 091301 (2007); S. Desai *et al.* [Super-K Collaboration], Phys. Rev. D **70**, 083523 (2004) [Erratum-ibid. D **70**, 109901 (2004)]; E. Behnke *et al.* [COUPP Collaboration], Science **319**, 933 (2008); G.J. Alner *et al.* [UKDM Collaboration], Phys. Lett. B **616**, 17 (2005).
- [53] A. Achterberg *et al.* [AMANDA Collaboration], Astropart. Phys. **26**, 129 (2006); M. Ackermann *et al.* [AMANDA Collaboration], Astropart. Phys. **24**, 459 (2006).
- [54] A. E. Erkoca, M. H. Reno and I. Sarcevic, in preparation.
- [55] G. Jungman and M. Kamionkowski, Phys. Rev. D **51**, 328 (1995); P. Lipari, Astropart. Phys. **1**, 195 (1993).